Movahediqomi, Mostafa; Vuyyuru, Sravan K. R.; Ptitcyn, Grigory; Valkonen, Risto; Kwon, Do-Hoon; Tretyakov, Sergei A.

Simultaneous Perfect Anomalous Reflection and Angle-of-Arrival Sensing Using Patch Arrays

Published in:
2024 IEEE International Symposium on Antennas and Propagation and INC/USNCURSI Radio Science Meeting, AP-S/INC-USNC-URSI 2024 - Proceedings

DOI:
10.1109/AP-S/INC-USNC-URSI52054.2024.10686489

Published: 19/07/2024

Document Version
Peer-reviewed accepted author manuscript, also known as Final accepted manuscript or Post-print

Please cite the original version:
Movahediqomi, M., Vuyyuru, S. K. R., Ptitcyn, G., Valkonen, R., Kwon, D.-H., & Tretyakov, S. A. (2024). Simultaneous Perfect Anomalous Reflection and Angle-of-Arrival Sensing Using Patch Arrays. In *2024 IEEE International Symposium on Antennas and Propagation and INC/USNCURSI Radio Science Meeting, AP-S/INC-USNC-URSI 2024 - Proceedings* (pp. 1497-1498). Article 10686489 (Digest of the IEEE Antennas and Propagation Society International Symposium). IEEE. https://doi.org/10.1109/AP-S/INC-USNC-URSI52054.2024.10686489

Simultaneous Perfect Anomalous Reflection and Angle-of-Arrival Sensing Using Patch Arrays

Mostafa Movahediqomi[1], Sravan K. R. Vuyyuru[1],[2], Grigory Ptitcyn[3], Risto Valkonen[2], Do-Hoon Kwon[4], and Sergei A. Tretyakov[1]

[1] Department of Electronics and Nanoengineering, School of Electrical Engineering, Aalto University, 02150 Espoo, Finland
[2] Nokia Bell Labs, Karakaari 7, 02610 Espoo, Finland
[3] Department of Electrical and Systems Engineering, University of Pennsylvania, Philadelphia, PA 19104, USA
[4] Department of Electrical and Computer Engineering, University of Massachusetts Amherst, Amherst, MA 01003, USA
(Emails: mostafa.movahediqomi@aalto.fi, sravan.vuyyuru@nokia.com)

***Abstract*—A novel optimization-based method tailored for the evolution of communication networks is presented, aimed at achieving a perfect power efficiency while accurately determining the angle of arrival of user-generated waves. Our approach involves optimizing aperiodic loaded structures, eliminating the constraints of electromagnetic periodicity while maintaining a fixed half-wavelength spacing. The proposed configuration employs practical square patches, each loaded with passive tunable elements. These load values can be dynamically adjusted, enabling a continuous scanning capability to capture user signals arriving from unknown angles.**

I. Introduction

Controlling the electromagnetic (EM) propagation environment using reconfigurable intelligent surfaces (RISs) can significantly impact the performance of communication networks for 6G advancements. Furthermore, multiple functionalities such as anomalous reflection and the angle-of-arrival (AoA) sensing using a single adjustable planar surface enhances the currently envisioned RISs [1], [2]. An intelligent EM surface can estimate the AoA for incoming waves from users, even when the directions are unknown. Recent research [3]–[5] has leveraged optimization methods to achieve an optimal power reflection efficiency even for redirecting the reflected wave at extreme angles, which contrasts with the poor efficiency of the conventional phase gradient approach.

In this work, we combine both functionalities to propose an impedance-loaded linear patch antenna array that can simultaneously redirect the incoming wave to an arbitrary angle (even extreme deflection) with a perfect power efficiency [5] and sense the AoA by optimizing the spatial Fourier spectrum of the surface current [6]. The key optimization parameters in our approach are the load impedances of the patches, which enable continuous tunability of the main scattering beam.

II. Methodology

Figure 1 illustrates a dual-functional RIS illuminated by a transverse electric (TE) wave from an unknown direction. Consider the case of a linear array of square patches on a grounded dielectric substrate. Each patch is terminated in a lumped load. In Fig. 1(a), the patch array is initially loaded with a set of random-valued N tunable impedances, Z_{Ln} $(n = 1, \ldots, N)$. This leads to random scattered fields, and the

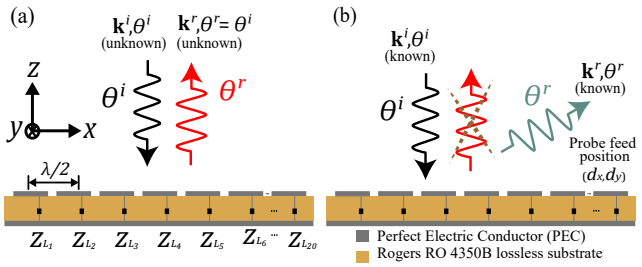

Fig. 1. Illustration of a dual-functional RIS comprising loaded patch elements. The stages depict (a) pre-optimization, featuring specular reflection from an unknown angle, and (b) post-optimization with perfect anomalous reflection and AoA estimation.

associated nonuniform current distribution at the loads ($\mathbf{I}_L$) [5] takes a vector form

$$\mathbf{I}_L = (\mathbf{Z}_A + \mathbf{Z}_L)^{-1} \mathbf{V}_{\text{oc}}, \tag{1}$$

where $\mathbf{V}_{\text{oc}}$ is the $N \times 1$ column vector representing voltages with disconnected loads at the patch terminals of the receiving (RX) antenna array. The load matrix $\mathbf{Z}_L$ is diagonal with reactive load values Z_{Ln}, and $\mathbf{Z}_A$ is the $N \times N$ input impedance matrix that includes both self-impedances (diagonal terms) and mutual impedances (symmetrical non-diagonal terms). The parameters $\mathbf{Z}_A$ and $\mathbf{V}_{\text{oc}}$ are computed using transmitting and RX full-wave EM simulations, respectively. Since the currents flow in negligibly small loads, the current distribution can be represented as a sum of spatial Dirac delta functions, corresponding to the positions shown in Fig. 1, i.e., $I_L(x) = I_1\delta(x) + I_2\delta(x-d) + \ldots + I_{20}\delta(x-19d)$ for a 20-element array. Using the spatial Fourier transform, the spectrum of the load current distribution can be found by a trivial calculation of the integral of delta functions as

$$\widehat{I}_{\text{L}}(k_x) = \sum_{n=1}^{20} I_{Ln} e^{-jk_x x_n}. \tag{2}$$

Here, I_m is the amplitude of the currents in each load wire, and $x_m = md$ are their x-coordinates.

In the next step, we aim to maximize the Fourier- transformed distribution of the load currents, $\mathscr{F}\{\mathbf{I}_L(x)\} = \widehat{\mathbf{I}}_L(k_x)$,

for a specific spatial harmonic that corresponds to the reflection angle as depicted in Fig. 1(b). The tangential wavevector or spatial frequency is $k_x = k \sin\theta$. Therefore, the objective function of the global optimization is defined as

$$\mathcal{O} = \max_{\mathbf{Z}_L} \{|\widehat{\mathbf{I}}_L(k \sin\theta_\mathrm{r})|\}. \tag{3}$$

Such a current spatial frequency generates a reflected plane wave at the desired angle. Importantly, in the optimized case, the patch current spectrum $\widehat{\mathbf{I}}_\mathrm{L}(k_x)$ will include one more strong peak at the spatial frequency $k_x = k \sin\theta_\mathrm{i}$, generated naturally and responsible for canceling out the structural scattering. As a result, we can detect the AoA by plotting the Fourier transform (FT) of the induced load current distribution.

III. Theoretical Results of Optimized Patch Arrays with a Half-Wavlength Spacing

As a simple example, we consider a linear array with an overall dimension of $10\lambda \times 0.5\lambda$ (λ = free-space wavelength) with a $\lambda/2$ element spacing containing 20 patch elements parallel with the x-axis, allowing for scanning in the xz-plane. Initially, a linearly polarized PEC square patch is tuned for a 50-Ω impedance match at 28 GHz. We employ a lossless Rogers RO4350B substrate (a relative permittivity of $\epsilon_r = 3.66$ and a thickness of 0.338 mm). The optimized patch length is 0.2385λ and the load position is $(d_x, d_y) = (0, 0.0415\lambda)$. We conduct full-wave EM simulations with CST Microwave Studio, obtaining the preliminary data of $\mathbf{Z}_A$ and $\mathbf{V}_\mathrm{oc}$ in preparation for global optimization [5].

Figure 2 shows the FT illustration of the spatial current distribution across the patch loads. As mentioned earlier, the optimization process results in the identification of two peaks in the propagation range between two black vertical lines. The primary peak is closely aligned with the green vertical line, achieving our objective of maximizing the rerouted power in that specific direction. The secondary peak, aligned with the red vertical line, signifies the direction of the incoming wave, emphasizing that an optimal solution incorporates a spatial harmonic for effectively canceling out the specular reflection. The peak outside the propagation range represents propagation along the surface as an evanescence wave.

The far-zone E-field distribution is depicted in Fig. 3, comparing cases of the optimized loads and the phase gradient loads employed as initial loads for optimization. Since the deflection angle is extremely wide compared with the incident angle, the reflected power to the desired direction is quite low for the initial loads. The optimized loads enhance the power density in the desired anomalous direction.

IV. Conclusions

A dual-functional RIS for AoA sensing and anomalous reflection has been presented. The main idea is to optimize the FT of the spatial current distribution for one specific spatial harmonic responsible for the reflection toward the desired angle where the receiver is located. In our future research, we aim to explore different objective functions to attain a super-directive solution and investigate the optimized performance and the AoA sensing accuracy with respect to the element spacing.

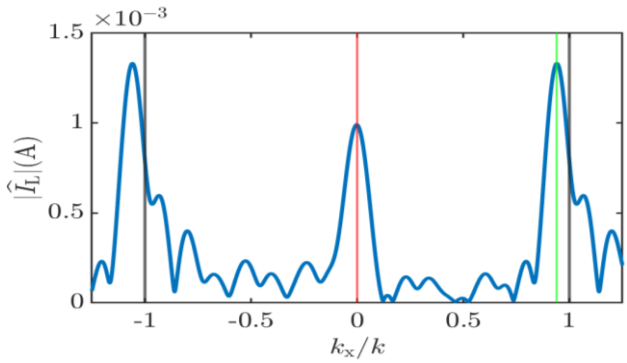

Fig. 2. The spatial spectrum of the optimized current. The green and red vertical lines correspond to the harmonics associated with the reflected and incident wave directions, respectively. Two black lines delineate the boundaries of the propagation range, where $k_x = \pm k$.

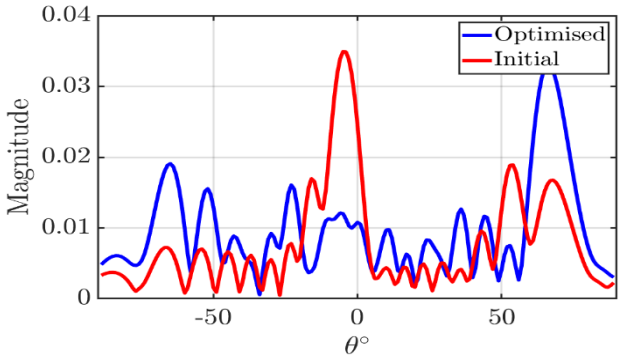

Fig. 3. Distribution of far-zone E-field before and after the optimization.

Acknowledgement

This work was supported by the European Union's Horizon 2020 MSCA-ITN-METAWIRELESS project under the Marie Skłodowska-Curie grant agreement No 956256 and the US Army Research Office under grant W911NF-19-2-0244.

References

[1] G. C. Alexandropoulos, N. Shlezinger, I. Alamzadeh, M. F. Imani, H. Zhang, and Y. C. Eldar, "Hybrid reconfigurable intelligent metasurfaces: Enabling simultaneous tunable reflections and sensing for 6g wireless communications," *IEEE Veh. Technol. Mag.*, pp. 2–11, 2023.

[2] H. Zhang, H. Zhang, B. Di, M. Di Renzo, Z. Han, H. V. Poor, and L. Song, "Holographic integrated sensing and communication," *IEEE J. Sel. Areas Commun.*, vol. 40, no. 7, pp. 2114–2130, Jul. 2022.

[3] M. Movahediqomi, G. Ptitcyn, and S. Tretyakov, "Comparison between different designs and realizations of anomalous reflectors for extreme deflections," *IEEE Trans. Antennas Propag.*, 2023.

[4] S. K. R. Vuyyuru, R. Valkonen, D.-H. Kwon, and S. A. Tretyakov, "Efficient anomalous reflector design using array antenna scattering synthesis," *IEEE Antennas Wireless Propag. Lett.*, vol. 22, no. 7, pp. 1711–1715, Jul. 2023.

[5] S. K. R. Vuyyuru, R. Valkonen, S. A. Tretyakov, and D.-H. Kwon, "Efficient synthesis of passively loaded finite arrays for tunable anomalous reflection," *arXiv preprint arXiv:2312.04441*, 2023.

[6] M. Movahediqomi, Y. Li, G. Ptitcyn, V. Asadchy, and S. A. Tretyakov, "Simultaneous high-efficiency anomalous reflection and angle of arrival sensing in reconfigurable intelligent surfaces," *arXiv preprint arXiv:2401.09864*, 2024.